Relativistic High-Energy Approximation for Elastic Scattering of Dirac Particles*

ADOLPH BAKER†
Brandeis University, Waltham, Massachusetts
(Received 17 September 1963, revised manuscript received 11 December 1963)

A high-energy approximation is described for predicting the elastic scattering of Dirac particles by a scalar potential. The formal solution is then applied to the specific problem of electron and positron scattering from nuclei. The predicted cross sections turn out to be in close agreement with those of partial-wave analysis, even for heavy nuclei and at large scattering angles, where the Born approximation is entirely inadequate.

I. INTRODUCTION AND SUMMARY

THE unsuitability of the first Born approximation for electron scattering from the heavier nuclei has been known for some time. The alternative method of phase-shift analysis has been successfully applied[1–4] to electron and positron scattering in the region of several hundred MeV, but as the energy increases the numerical difficulties tend to proliferate rapidly. Furthermore, the division of the problem into solution of separate partial waves may tend at times to obscure one's contact with the underlying physics.

Several attempts have been made to provide a suitable approximation technique for the heavy elements, but so far these have appeared too limited in their range of usefulness to attain general acceptance or application. A high-energy approximation for the Schrödinger equation was shown by Glauber[5] to have a range of validity which encompasses that of both Born approximation and the WKB method, as well as the region in between. Schiff,[6] using the method of stationary phase, also made such an approximation, not only for the Schrödinger equation, but for the Dirac equation as well. He developed two approximations, one valid for small scattering angles, and the other for large angles. Because his derivation of the small-angle approximation suggested that it was valid over only an extremely small angular range, it was rather his large-angle formula which was applied in asymptotic form by Tiemann[7] with somewhat limited success to the same nuclear model as in Figs. 2, 3, and 4 below. Since an intermediate range of angles had apparently not been included, subsequent developments by Saxon[8,9] and Schiff[9] extended the treatment to include all angles, with the small angle formula as a simplifying limit.

In this paper an independent theoretical development by another method has resulted in the same expression which Schiff obtained for small angles, but suggests that it is accurate over a much greater range of angles than his derivation implied. It is then shown how this simple result may be applied to specific models, giving close agreement with partial-wave calculations over the entire angular range.

The method taken here follows the approach of Glauber,[5] who solved the Schrödinger equation for scattering in the high-energy limit by introducing into the expression for the scattering amplitude a wave function which consists of a plane wave modulated by a slowly varying function of position. Now, however, it is the Dirac equation which is to be solved, the plane wave becomes a spinor, and the slowly varying function becomes a 4×4 matrix operator in the space of the Dirac matrices.

The formal result turns out finally to be fairly simple, resembling that for the Schrödinger equation, and differing in fact only by the added presence of a spinor term. The expression for the scattering amplitude is an integral over a variable related to the classical impact parameter, replacing the summing of discrete partial waves.

This result has been applied to the problem of the scattering of electrons and positrons from an arbitrary (spherically symmetric) nuclear model. The final integral expression for the scattering amplitude consists of two parts, one a single integration within the nuclear charge cloud, and the other corresponding to those particles whose classical orbits pass through the purely Coulomb region outside the nucleus. The latter integration has been carried out explicitly in terms of known functions, while the former must in general be evaluated numerically for an arbitrary charge distribution.

In addition to calculations carried out for comparison with phase-shift techniques, a cross section has also been computed for the scattering of 1000 MeV electrons from a uniform model gold nucleus. At this energy, where for numerical reasons phase-shift analysis becomes extremely unwieldy, if at all usable, the high-energy approximation continues to give stable results, and in fact increases in validity. The relatively simple

---

* This paper is based on a doctoral dissertation submitted to Brandeis University in August 1963. The research was supported by the U. S. National Science Foundation.
† Present address: Lowell Technological Institute, Lowell, Massachusetts.
[1] R. Hofstadter, Ann. Rev. Nucl. Sci. **7**, 238 (1957).
[2] D. G. Ravenhall and D. R. Yennie, Proc. Phys. Soc. (London) **70**, 857 (1957).
[3] U. Meyer-Berkhout, K. W. Ford, and A. E. S. Green, Ann. Phys. (N. Y.) **8**, 129 (1959).
[4] R. Herman, B. C. Clark, and D. G. Ravenhall (unpublished).
[5] R. J. Glauber, in *Lectures in Theoretical Physics* (Interscience Publishers, Inc., New York, 1959), Vol. I.
[6] L. I. Schiff, Phys. Rev. **103**, 443 (1956).
[7] J. J. Tiemann, Phys. Rev. **109**, 183 (1958).
[8] D. S. Saxon, Phys. Rev. **107**, 871 (1957).
[9] D. S. Saxon and L. I. Schiff, Nuovo Cimento **6**, 614 (1957).

functional form of the scattering matrix element may also be expected to improve one's insight into the scattering processes and target structure.

II. SOLUTION OF THE DIRAC EQUATION IN THE HIGH-ENERGY APPROXIMATION

We begin by considering the Dirac equation for a particle in the presence of a scalar potential $V(\mathbf{r})$,

$$(\boldsymbol{\alpha}\cdot\mathbf{p}+\beta m-E)\psi(\mathbf{r})=-V(\mathbf{r})\psi(\mathbf{r})\,, \tag{1}$$

in the natural system of units where $\hbar=c=1$. E and m are energy and mass of the incident particle, respectively, and $\boldsymbol{\alpha}$ and β are of course the Dirac matrices. The Green's function for this equation is likewise a 4×4 matrix in the space of Dirac operators, and may be used to obtain the scattering solution,

$$\psi(\mathbf{r})=u_0(\mathbf{k}_0)e^{i\mathbf{k}_0\cdot\mathbf{r}}-\frac{1}{4\pi}\int(\boldsymbol{\alpha}\cdot\mathbf{p}+\beta m+E)\times\frac{e^{ik|\mathbf{r}-\mathbf{r}'|}}{|\mathbf{r}-\mathbf{r}'|}V(\mathbf{r}')\psi(\mathbf{r}')d\mathbf{r}'\,. \tag{2}$$

The incident plane-wave spinor $u_0(\mathbf{k}_0)$ is a function of the incident momentum $\mathbf{k}_0$, ψ is a spinor, and $\mathbf{p}=-i\nabla_r$ operates with respect to $\mathbf{r}$.

Asymptotically, far from the scattering center,

$$\psi(\mathbf{r})\sim u_0(\mathbf{k}_0)e^{i\mathbf{k}_0\cdot\mathbf{r}}-\frac{1}{4\pi}(\boldsymbol{\alpha}\cdot\mathbf{k}_f+\beta m+E)\frac{e^{ikr}}{r}\times\int e^{-i\mathbf{k}_f\cdot\mathbf{r}'}V(\mathbf{r}')\psi(\mathbf{r}')d\mathbf{r}'\,, \tag{3}$$

where $\mathbf{k}_f$ is the final-state momentum. The scattering amplitude is therefore a spinor and is given by

$$f(\theta)=-\frac{1}{4\pi}(\boldsymbol{\alpha}\cdot\mathbf{k}_f+\beta m+E)\int e^{-i\mathbf{k}_f\cdot\mathbf{r}}V(\mathbf{r})\psi(\mathbf{r})d\mathbf{r}\,. \tag{4}$$

The matrix element for scattering in the direction θ with a particular spin state is, however, a scalar obtained by forming the inner product of $f(\theta)$ with the Hermitian adjoint of the final-state spinor. Thus the matrix element for this transition is

$$M=u_f^*(\mathbf{k}_f)f(\theta)\,. \tag{5}$$

Following now the approach taken by Glauber[5] in the high-energy approximation for the Schrödinger equation, we assume a solution for the wave function in Eq. (2) in the form of a plane-wave spinor modulated by a slowly varying function of position. Thus

$$\psi(\mathbf{r})=\varphi(\mathbf{r})u_0(\mathbf{k}_0)e^{i\mathbf{k}_0\cdot\mathbf{r}}, \tag{6}$$

where $\varphi(r)$ is the modulating function, in this case a 4×4 matrix operator.

Substituting Eq. (6) in Eq. (2) enables us to obtain an expression for $\varphi(r)$.

$$\varphi(\mathbf{r})=1-\frac{1}{4\pi}\int e^{-i\mathbf{k}_0\cdot\mathbf{r}''}(\boldsymbol{\alpha}\cdot\mathbf{p}+\beta m+E)\frac{e^{ikr''}}{r''}\times V(\mathbf{r}-\mathbf{r}'')\varphi(\mathbf{r}-\mathbf{r}'')d\mathbf{r}''\,, \tag{7}$$

where $\mathbf{r}''=\mathbf{r}-\mathbf{r}'$, and the first term on the right is the unit matrix.

We now introduce the restriction that $V\varphi$ vary by a small fractional amount over a reduced particle wavelength $1/k$. This is an important restriction on both the potential and the modulating function. The effect of a violation of this condition will be seen subsequently. We can further express this limitation by noting that if d is a distance over which $V\varphi$ varies significantly, then $1/kd\ll1$. The high-energy approximation is a process of dropping higher order terms in $1/kd$.

We consider first the integration of that portion of Eq. (7) which does not involve the gradient operator $\mathbf{p}$. Integrating by parts in spherical coordinates over $\mu=\cos\theta$, it may be seen that the expression is of the form

$$\int_0^\infty\int_{-1}^{+1}r''F(\mu)e^{ikr''(1-\mu)}d\mu dr''=\int_0^\infty\left[\frac{F(\mu)e^{ikr''(1-\mu)}}{-ik}\right]_{\mu=-1}^{\mu=+1}dr''+\frac{1}{ik}\times\int_0^\infty\int_{-1}^{+1}F'(\mu)e^{ikr''(1-\mu)}d\mu dr''\,, \tag{8}$$

where $F(\mu)\sim V\varphi$ has been so written because here we are interested only in its μ dependence. This portion of the solution corresponds to that of the Schrödinger equation, and it has been observed[5] that the final term of Eq. (8), as well as the lower limit $\mu=-1$, contribute expressions $O(1/kd)$ which may be dropped, leaving only the $\mu=+1$ term. This may be readily adduced by considering piecewise integration over r'' in intervals of length d.

There remains the $\boldsymbol{\alpha}\cdot\mathbf{p}$ term in Eq. (7). This may be written

$$\sim\int_{-1}^{+1}d\mu\boldsymbol{\alpha}\cdot\hat{n}''\int_0^\infty dr''(ik-1/r'')r''\times e^{ikr''(1-\mu)}V(\mathbf{r}-\mathbf{r}'')\varphi(\mathbf{r}-\mathbf{r}'')\,, \tag{9}$$

where $\hat{n}''=\mathbf{r}''/r''$. Now the $1/r''$ term in Eq. (9) is $O(1/kd)$ compared to the ik term, and may likewise be neglected by the same reasoning, although here this is apparent before the integration by parts.

Thus in the high-energy limit, assuming cylindrical

symmetry about the z axis, Eq. (7) becomes

$$\varphi(\mathbf{r})=1-\frac{i}{2k}\int_0^\infty(\boldsymbol{\alpha}\cdot k\hat{n}''+\beta m+E)\times V(\mathbf{r}-\mathbf{r}'')\varphi(\mathbf{r}-\mathbf{r}'')\Big|_{\mu=+1}dr'', \quad (10)$$

where the retention of only the $\mu=+1$ term in Eq. (8) requires that the integration be carried out subject to the condition that $\mathbf{r}''$ remain parallel to $\hat{z}$, the unit vector in the z direction. In Cartesian coordinates,

$$\varphi(x,y,z)=1-\frac{i}{2k}(\boldsymbol{\alpha}\cdot k\hat{z}+\beta m+E)\times\int_{-\infty}^{z}V(x,y,z')\varphi(x,y,z')dz'. \quad (11)$$

This integral equation may be solved, giving

$$\varphi(x,y,z)=\exp\left[-\frac{i}{2k}(\boldsymbol{\alpha}\cdot k\hat{z}+\beta m+E)\times\int_{-\infty}^{z}V(x,y,z')dz'\right]. \quad (12)$$

Since we have taken the z axis in the direction of the incoming momentum vector, the wave function of Eq. (6) becomes

$$\psi(\mathbf{r})=\exp\left\{i\left[\mathbf{k}_0\cdot\mathbf{r}-\frac{1}{2k}(\boldsymbol{\alpha}\cdot\mathbf{k}_0+\beta m+E)\times\int_{-\infty}^{z}V(x,y,z')dz'\right]\right\}u_0(\mathbf{k}_0). \quad (13)$$

But the initial-state spinor is an eigenfunction of $(\boldsymbol{\alpha}\cdot\mathbf{k}_0+\beta m+E)$ with eigenvalue $2E$, so that

$$\psi(\mathbf{r})=\exp\left\{i\left[\mathbf{k}_0\cdot\mathbf{r}-\frac{E}{k}\int_{-\infty}^{z}V(x,y,z')dz'\right]\right\}u_0(\mathbf{k}_0). \quad (14)$$

The matrix element Eq. (5) therefore becomes, upon substituting Eq. (14) into Eqs. (4) and (5),

$$M=-\frac{1}{4\pi}u_f^*(\mathbf{k}_f)(\boldsymbol{\alpha}\cdot\mathbf{k}_f+\beta m+E)u_0(\mathbf{k}_0)\times\int\exp\left\{i\left[\mathbf{q}\cdot\mathbf{r}-\frac{E}{k}\int_{-\infty}^{z}V(x,y,z')dz'\right]\right\}\times V(\mathbf{r})d\mathbf{r}, \quad (15)$$

where $\mathbf{q}$ is the momentum transfer $\mathbf{k}_0-\mathbf{k}_f$.

The final-state spinor is likewise an eigenfunction of the Dirac operator in Eq. (15), operating to the left

Therefore, transforming to cylindrical coordinates,

$$M=-\frac{E}{2\pi}u_f^*u_0\int\exp[i\mathbf{q}\cdot(\mathbf{b}+\hat{z}z)]V(\mathbf{b},z)\times\exp\left[-i\frac{E}{k}\int_{-\infty}^{z}V(\mathbf{b},z')dz'\right]dzd^{(2)}b, \quad (16)$$

where $d^{(2)}b$ designates integration over the plane of impact vectors, and $\mathbf{b}$ represents the classical impact parameter.

Equation (16) has a significant defect. It is not symmetric under velocity reversal. This is due to the nature of the trial function Eq. (6), which singled out the incoming momentum vector for preferential treatment. Thus our solution in its present form requires a further adjustment if it is to have the important property of time reversal invariance. A simple step for restoring this symmetry is to effect a coordinate rotation of Eq. (16) through angle $\theta/2$, where θ is the scattering angle, so that the incoming and outgoing momentum vectors both made an angle $\theta/2$ to the z direction. The spinor product of course remains invariant, but the integral is changed in value. In the new coordinate system,

$$\exp(i\mathbf{q}\cdot\hat{z}z)=1, \quad (17)$$

since the momentum transfer vector is now perpendicular to the z axis. This same coordinate rotation was introduced in Glauber's solution[5] of the Schrödinger equation. It is interesting that as an alternative to the somewhat arbitrary change of direction, the same result is obtained from Eq. (16) if we make a small-angle approximation. Thus, if we restrict the solution to small scattering angles, Eq. (17) becomes approximately correct for the original coordinate system. The restriction on angles, however, is quite severe, and may be shown to be

$$\theta^2\ll 1/kR, \quad (18)$$

where R is of the order of the target radius. It will be seen subsequently that the final solution suffers no such limitation.

As a result of our choice of a symmetric coordinate system, it now becomes possible to integrate Eq. (16) with respect to z, resulting in

$$M=\frac{k}{2\pi i}u_f^*u_0\int e^{i\mathbf{q}\cdot\mathbf{b}}\times\left[\exp\left\{-i\frac{E}{k}\int_{-\infty}^{\infty}V(\mathbf{b},z')dz'\right\}-1\right]d^{(2)}b. \quad (19)$$

Since now

$$\mathbf{q}\cdot\mathbf{b}=qb\cos\varphi, \quad (20)$$

where φ is the azimuthal angle in cylindrical coordinates, in the case of problems with spherical symmetry we may formally integrate Eq. (19) over angles by employing the integral representation of the Bessel

function. Thus, finally, the matrix element for transitions from initial to final plane-wave spinor states is given by

$$M=\frac{k}{i}u_f^*u_0\int_0^\infty J_0(qb)[e^{i\chi(b)}-1]bdb, \quad (21)$$

where

$$\chi(b)=-\frac{E}{k}\int_{-\infty}^{\infty}V(b,z)dz, \quad (22)$$

differing from Glauber's result only in the presence of the spinor product $u_f^*u_0$. This term now incorporates into the high-energy approximation the effect of both spin and relativity, although no additional approximating conditions have had to be introduced.

Equation (21) is identical to the result obtained by Schiff[6] as a small-angle approximation, using a somewhat different though not unrelated approach. Despite the *ad hoc* character of the introduction of time-reversal symmetry in going from Eqs. (16) to (19), it seems preferable to making a small-angle assumption in this final stage of the derivation. One would understandably be led to assume that a restriction of the nature of Eq. (18) invalidates the usefulness of this result, particularly as a high-energy approximation. However, the application of Eq. (21) in Sec. V below to various nuclear targets and energies shows no evidence of degradation in accuracy even at large scattering angles. This would appear to justify the viewpoint that the arbitrary introduction of a symmetric coordinate system represents a restoration of accuracy rather than an added approximation. This is further adduced by the relationship the result bears to the Born approximation. If the second exponential factor in Eq. (19) is expanded, the leading term is

$$M^{(1)}=-\frac{E}{2\pi}u_f^*u_0\int e^{iqb\cos\varphi}V(b,z)bdbdzd\varphi, \quad (23)$$

which, for spherically symmetric potentials, is identical to the first Born approximation, since $qb\cos\varphi=\mathbf{q}\cdot\mathbf{r}$. Thus, the high-energy approximation is equivalent to an infinite Born expansion, in which the first Born term is precisely duplicated, while all the higher order terms are approximated.

The scattering amplitude thus employs a wave function which has been modulated in phase by the presence of the force field. However, there is yet another effect which has not been included, namely, a type of frequency modulation which reduces the de Broglie wavelength of the incident particle as it acquires kinetic energy upon approaching the scattering center. This effect has been observed[10,11] in electron scattering phenomena as a shift in the diffraction zeros of Born approximation in the direction of increased scattering angles. Since the particle's wavelength is its meter stick for exploring the target, any approximation which fails to take account of this contraction will observe things to be larger than they actually are. The basic dimensionless parameter of the problem is the product of length times momentum transfer [appearing in Eq. (21) as the argument of the Bessel function], and an increase in length therefore corresponds to increased momentum transfer, viz., larger scattering angles. Conversely if we wish to duplicate the correct scattering cross section, we must increase all length dimensions by a suitable factor. This factor should be roughly the particle wavelength at infinity divided by some average wavelength in the scattering region. A reasonable factor which seems to work fairly well for electron scattering is the kinetic energy as computed at the rms radius of the target charge distribution, divided by the incident energy, that is, $[1+|V(r_{\rm rms})|/E]$. The effect is not large enough to be very critical, amounting to approximately a five percent increase in length dimensions for 400-MeV electrons scattered by heavy nuclei. In the limit of very high energies the correction becomes insignificant.

III. THE COULOMB POTENTIAL

We turn now to the application of the high-energy approximation to Coulomb interactions. In order to evaluate the $\chi(b)$ function of Eq. (22) for scattering of electrons by a Coulomb potential, it is necessary for the usual physical and mathematical reasons to introduce a screen, which is subsequently moved an arbitrarily large distance from the scattering center. This has been done most conveniently[5] with a step function cutoff at the screen distance a, resulting, for an attractive potential, in

$$\begin{aligned}\chi(b)&=2\alpha Z\frac{E}{k}\ln\left(\frac{a+(a^2-b^2)^{1/2}}{b}\right), && b\leq a\\ &= 0, && b\geq a,\end{aligned} \quad (24)$$

where α is the fine structure constant and Z is the nuclear charge.

Expanded for large a in powers of b/a,

$$\chi(b)=-2\alpha Z(E/k)\ln(b/2a), \quad (25)$$

plus successively higher powers of b/a which vanish in the limit as the screen distance a goes to infinity.

When Eq. (25) is substituted in Eq. (21), the resulting definite integral may be evaluated,[12,5] provided a damping exponential is first introduced for purpose of convergence and then allowed to approach unity. The matrix element for Coulomb scattering by an attractive potential becomes

$$M_c=\frac{2\alpha ZE}{q^2}\exp\left\{i\left[2\alpha Z\frac{E}{k}\ln qa+2\eta\right]\right\}u_f^*u_0, \quad (26)$$

[10] R. Hofstadter, Rev. Mod. Phys. **28**, 219 (1956).

[11] B. W. Downs, D. G. Ravenhall, and D. R. Yennie, Phys. Rev. **106**, 1285 (1957).

[12] G. N. Watson, *Theory of Bessel Functions* (Cambridge University Press, New York, 1952), 2nd ed., pp. 385, 190, 350, 351, 345, 347, 194, 195.

where $\eta=\arg\Gamma(1-\alpha ZiE/k)$, and the momentum transfer $q=2k\sin(\theta/2)$.

If we are not interested in the polarization of the electron, then the spinor term, which in the expression for the differential cross section appears as $|u_f^*u_0|^2$, may be averaged over initial spin states and summed over final states in the usual manner by the method of traces.[13] For extremely relativistic particles, if the mass of the incident particle is neglected compared to its energy, this turns out to be[1] simply

$$|u_f^*u_0|^2=\cos^2(\theta/2)\,. \tag{27}$$

Without the spinor-produced term $\cos^2(\theta/2)$, which introduces spin and relativity, this results in the familiar Rutherford cross section. Furthermore, even the logarithmic phase factor which characterizes the exact nonrelativistic solution[14,15] is present in the scattering amplitude (subject to adjustment of the arbitrary screen parameter a). One is therefore inclined to draw considerable comfort from the nonrelativistic form of Eq. (26) as a verification of the validity of the high-energy approximation.

But when the spinor term is reinstated, and Eq. (26) is regarded as a solution for Dirac particles, this comfort turns out to be short-lived. What we have is the first Born cross section, which is correct relativistically only in the limit $\alpha Z\ll 1$, and has been found[1,10] to be inadequate for scattering from a point charge corresponding to one of the heavier nuclei.

This result should, however, come as no surprise, since the high-energy approximation is based on the premise that the potential varies little over a particle wavelength, and this condition has been violated in the case of the Coulomb potential by the singularity at the origin. Since the first term of the Born series is precisely reproduced in this approximation, it comes through in any case, but the higher order terms are not adequately represented.

Thus a valid test of this technique can be made for Coulomb interactions only when the target has finite extent. This will therefore now be considered.

IV. SCATTERING BY A CHARGE CLOUD—THE SCATTERING OF HIGH-ENERGY ELECTRONS AND POSITRONS FROM NUCLEI

A. The χ Function for an Arbitrary Spherically Symmetric Charge Distribution

For simple models, such as the shell and the sphere, the integration of Eq. (22) is easily carried out. This is not, however, always the case, particularly when the potential may not be written as an explicit function of position. It is therefore convenient to express $\chi(b)$ in terms of the charge distribution. To do this we utilize the Coulomb result Eq. (25) for a charge element, and integrate over the nuclear charge cloud.

Introducing the relative coordinate ξ of a field point $\mathbf{r}$ with respect to a charge point $\mathbf{R}$, and the spherically symmetric charge distribution $\rho(R)$ normalized to unity,

$$\xi=\mathbf{r}-\mathbf{R}\,,$$

$$\chi(b_r)=-\frac{E}{k}\int d\mathbf{R}\,\rho(R)\int_{-\infty}^{\infty}V(\mathbf{b}_\xi,z_\xi)dz_\xi\,, \tag{28}$$

where subscripts have been introduced to distinguish coordinate systems, and we define a relative variable $\mathbf{b}_\xi$ in cylindrical coordinates such that

$$b_\xi^2=b_R^2+b_r^2-2b_rb_R\cos\varphi. \tag{29}$$

Employing the Coulomb solution Eq. (25) in Eq. (28),

$$\chi(b_r)=-2\alpha Z\frac{E}{k}\int d\mathbf{R}\,\rho(R)\ln\frac{b_\xi}{2a}\,. \tag{30}$$

Upon the substitution of Eq. (29) in Eq. (30), the latter may be integrated over polar angle in cylindrical nuclear coordinates, with the result

$$\chi(b_r)=-4\pi\alpha Z\frac{E}{k}\left\{\ln\frac{b_r}{2a}\int_0^{b_r}b_RF(b_R)db_R+\int_{b_r}^{\infty}b_R\ln\frac{b_R}{2a}F(b_R)db_R\right\}, \tag{31}$$

where

$$F(b_R)=\int_{-\infty}^{\infty}\rho(\mathbf{b}_R,z_R)dz_R\,. \tag{32}$$

It is sometimes convenient to evaluate the "form function" $F(b_R)$ for a particular model, and then introduce it in Eq. (31). Alternately it is illuminating to write $\chi(b)$ as the volume integral

$$\chi(b)=-2\alpha Z\frac{E}{k}\left\{\ln\frac{b}{2a}\int_{b'=0}^{b'=b}\rho(r')d\tau'+\int_{b'=b}^{\infty}\ln\frac{b'}{2a}\rho(r')d\tau'\right\}, \tag{33}$$

where subscripts have been dropped, and the first integral of Eq. (33) is evaluated within a cylinder of radius b, while the second is evaluated outside this cylinder.

It is interesting to compare Eq. (33) with the corresponding expression for the potential,

$$V(r)=-\alpha Z\left\{\frac{1}{r}\int_0^r\rho(r')d\tau'+\int_r^{\infty}\frac{1}{r'}\rho(r')d\tau'\right\}. \tag{34}$$

Thus, the $\chi(b)$ function in the high-energy approxima-

[13] S. S. Schweber, *Introduction to Relativistic Quantum Field Theory* (Row-Peterson, Inc., Evanston, Illinois, 1961), pp. 87–90.
[14] N. F. Mott and H. S. W. Massey, *Theory of Atomic Collisions* (Oxford University Press, New York, 1949), 2nd ed., p. 48.
[15] L. I. Schiff, *Quantum Mechanics* (McGraw-Hill Book Company, Inc., New York, 1955), 2nd ed., p. 116.

tion contains all the necessary information about the scattering center, and its determination corresponds to that of the potential in other forms of analysis.

The peculiar mixture of spherical with cylindrical symmetry in Eq. (33) may, however, be further simplified. Taking advantage of the normalization of the charge density $\rho(r')$, Eq. (33) may be written

$$\chi(b)=-2\alpha Z\frac{E}{k}\left\{\ln\frac{b}{2a}+\int_{b'=b}^{\infty}\ln\frac{b'}{b}\rho(r')d\tau'\right\}. \quad (35)$$

The remaining integral in Eq. (35) may then be integrated over angles in spherical coordinates, since

$$\int_{b'=b}^{\infty}\ln\frac{b'}{b}\rho(r')d\tau'=4\pi\int_{b}^{\infty}dr'r'^2\rho(r')\times\int_0^{[1-(b/r')^2]^{1/2}}d\mu'\ln\frac{r'(1-\mu'^2)^{1/2}}{b}, \quad (36)$$

where $\mu'=\cos\theta'$, and the cylindrical integration limits have been expressed in spherical form. When the integration over μ' is carried out,

$$\chi(b)=-2\alpha Z\frac{E}{k}\left\{\ln\frac{b}{2a}+4\pi\int_{b}^{\infty}dr'\rho(r')r'^2\times\left[\ln\frac{1+[1-(b/r')^2]^{1/2}}{b'/r'}-[1-(b/r')^2]^{1/2}\right]\right\}. \quad (37)$$

Thus the cylindrically symmetric function $\chi(b)$ is written as a single spherically symmetric integral over the charge density. It may in fact be expressed as

$$\chi(b)=-2\alpha Z\frac{E}{k}\left\{\ln\frac{b}{2a}+\langle f(b/r)\rangle\right\}, \quad (38)$$

dropping the primes, where

$$f(b/r)=\ln\frac{1+[1-(b/r)^2]^{1/2}}{b/r}-[1-(b/r)^2]^{1/2}, \quad (39)$$

and $\langle f(b/r)\rangle$ is the mean value of this function, weighted by the charge distribution and evaluated over all $r\geq b$. The function $f(b/r)$ is independent of the nuclear structure, and reflects only the Coulombic character of the interaction between the incoming particle and an element of the charge cloud.

The infinite upper limit of integration in Eq. (37) may be replaced by R_0, the cutoff radius of the charge distribution, i.e., the point beyond which the charge density vanishes or becomes negligible, and a pure Coulomb potential exists. Then the integral in Eq. (37) is defined only for $b\leq R_0$, and vanishes for all $b>R_0$, where Eq. (37) becomes simply Eq. (25).

It is convenient further to remove from $\chi(b)$ the singularity resulting from the infinitely large screen parameter a. This may be done without loss of generality by so choosing the arbitrary screen distance a that

$$2\alpha Z(E/k)\ln(R_0/2a)=2\pi n, \quad (40)$$

where n is an integer. As the screen is moved to infinity the distance a is increased in discrete jumps so that Eq. (40) is always satisfied. This enables us to drop this phase factor when $\chi(b)$ is inserted in Eq. (21), so that finally

$$\chi(b)=-2\alpha Z\frac{E}{k}\left\{\ln\frac{b}{R_0}+4\pi\int_{b}^{R_0}dr\rho(r)r^2f(b/r)\right\}, \quad b\leq R_0, \quad (41)$$

and

$$\chi(b)=-2\alpha Z\frac{E}{k}\ln\frac{b}{R_0}, \quad b\geq R_0. \quad (42)$$

B. Explicit Evaluation of $\chi(b)$ for Physical Models

Outside the charge cloud Eq. (42) of course applies. It is therefore only necessary to integrate Eq. (41) for the region inside the nucleus.

1. Shell

Here

$$\rho(r)=\delta(r-R_0)/4\pi R_0^2$$

and

$$\chi(b)=-2\alpha Z\frac{E}{k}\{\ln[1+(1-(b/R_0)^2)^{1/2}]-[1-(b/R_0)^2]^{1/2}\}. \quad (43)$$

2. Uniform Sphere

$$\rho(r)=3/4\pi R_0^3,$$

$$\chi(b)=-2\alpha Z(E/k)\{\ln[1+(1-(b/R_0)^2)^{1/2}]-\tfrac{1}{3}[4-(b/R_0)^2][1-(b/R_0)^2]^{1/2}\}. \quad (44)$$

3. Harmonic Oscillator Potential (Shell Model)

$$\rho(r)=(A+Br^2)e^{-\lambda^2r^2}.$$

This case is most readily solved by means of Eq. (31).

$$\chi(b)=-2\alpha Z\frac{E}{k}\left\{\left(C+\frac{D}{\lambda^2}\right)\times\left[\ln\frac{b}{R_0}-Ei(-\lambda^2b^2)/2\right]+\frac{D}{2\lambda^2}e^{-\lambda^2b^2}\right\}, \quad (45)$$

where

$$C=(\sqrt{\pi}/\lambda)(A+B/2\lambda^2),$$
$$D=B\sqrt{\pi}/\lambda,$$

and $Ei(-\lambda^2b^2)$ is the exponential integral.

When none of the equations (22), (31), or (41) can be explicitly integrated, it becomes necessary to evaluate Eq. (41) by numerical integration. This process corresponds to the integration of Eq. (34) for

the potential when the latter cannot be expressed as an explicit function of position.

C. The Scattering Amplitude

The prediction of scattering cross sections finally becomes the problem of evaluating the integral (21) for a given charge density distribution. Since the integrand is an oscillating function whose amplitude diverges asymptotically as the square root of the argument, the integral is defined only with exponential damping, as in the case of the Coulomb solution. This effectively precludes the possibility of any numerical integration schemes for evaluating the infinite integral. However, if we break Eq. (21) into two parts, one for $b\leq R_0$, the nuclear cutoff radius, and the other corresponding to the Coulomb region $b\geq R_0$, the latter integration may be explicitly carried out to infinity.

Before performing this integration, it should be noted that the second term of Eq. (21) in brackets, consisting of unity, vanishes for $\theta\neq 0$ when integrated over the entire range zero to infinity, subject of course to the introduction of the negative exponential. It is therefore tempting to drop this term, dividing the remaining expression into the two ranges of integration. This would, however, be an unfortunate decision, as will subsequently become apparent, since if retained this term will cancel precisely another large term in the explicit solution of the model-independent integral over $b\geq R_0$. Failure to observe this explicit cancellation would relegate it to numerical evaluation, resulting in error amplification of several orders of magnitude arising from the differencing of large numbers.

The integral in Eq. (21) may be written, omitting the spinor product, as

$$I=I_1+I_2, \tag{46}$$

where, letting $x=b/R_0$,

$$I_1=\frac{kR_0^2}{i}\int_0^1 J_0(qR_0x)[e^{i\chi(x)}-1]xdx, \tag{47}$$

$$I_2=\frac{kR_0^2}{i}\int_1^\infty J_0(qR_0x)[e^{-2\alpha Zi\,\ln x}-1]xdx, \tag{48}$$

and the factor E/k has been made unity here and in the following equations, corresponding to extremely relativistic particles. $\chi(x)$ is defined only for $x\leq 1$, and is in general obtained from Eq. (41) expressed as a function of b/R_0. Equation (48) may be integrated (see Appendix), with the result

$$\begin{aligned}I_2=-\frac{k}{iq^2}[&e^{2\alpha Zi\,\ln qR_0}\\&\times\{-2\alpha ZiqR_0J_0(qR_0)S_{-2\alpha Zi,\,-1}(qR_0)\\&+qR_0J_1(qR_0)S_{1-2\alpha Zi,\,0}(qR_0)\}\\&-qR_0J_1(qR_0)],\end{aligned} \tag{49}$$

where J_0 and J_1 are Bessel functions, and $S_{\mu\nu}$ are Lommel's functions.[12]

In order to obtain a numerical result for I_2 it is necessary to employ the asymptotic series Eq. (A5) for $S_{\mu\nu}(qR_0)$. If the cutoff radius R_0 is made sufficiently large that

$$qR_0\gtrsim 10, \tag{50}$$

then the retention of the first three terms of the series insures accuracy of better than one part in 2000. There is little merit in going beyond three terms, and if one includes too many terms the situation becomes worse due to the divergence of the series. The requirement Eq. (50) actually turns out to be quite reasonable for physically interesting models.

It may now be seen why it was important to retain the unity term in Eq. (48), resulting in the last term of Eq. (49). This term cancels precisely the first term (unity) in the asymptotic expansion of $S_{1-2\alpha Zi,\,0}(qR_0)$, when it is inserted into the next to the last term of Eq. (49).

Since asymptotically $qR_0J_1(qR_0)\sim(qR_0)^{1/2}$, this term would increase with cutoff radius. Its contribution to I_2 for typical nuclear radius and energy would represent a term in the cross section whose order of magnitude is comparable to or greater than that for a Coulomb point charge, and is larger by some decades than the solution for a distributed charge (see Figs. 21 and 22 of Ref. 1). Thus if this term were present in the solution we would have

$$|I_2|\gg|I_1+I_2|. \tag{51}$$

Since I_1 must in general be computed numerically, errors in numerical integration would be amplified as much as 100 times in the scattering amplitude. The explicit cancellation of this undesirable term avoids such large numerical cancellations, making it possible to apply the high-energy approximation to energies well up in the BeV range.

All terms of Eq. (49) which remain after this explicit cancellation decrease with increase in R_0, so that the situation represented by Eq. (51) may be avoided or at least minimized by choosing R_0 sufficiently large. The integration of I_1 in Eq. (47) is in general carried out numerically, and the result added to Eq. (49). The alternation of the positive and negative Bessel loops in the integrand of Eq. (21) provides the mathematical correspondence to the process which occurs when the separate partial waves are added. It is interesting also to note that our explicit evaluation of I_2 to infinity corresponds to summing all the phases, whereas the partial-wave expansion must be terminated in practice.

In choosing a convenient value of cutoff radius R_0, one should remember to satisfy Eq. (50); otherwise the asymptotic series Eq. (A5) is not suitable for obtaining the Lommel's functions $S_{\mu\nu}$. Thus calculations for the uniform model in the 200–300-MeV region were based

on a modified form of Eq. (44),

$$\chi(b)=-2\alpha Z\frac{E}{k}\left\{\ln\frac{r_1}{R_0}+\ln[1+(1-(b/r_1)^2)^{1/2}]-\tfrac{1}{3}[4-(b/r_1)^2][1-(b/r_1)^2]^{1/2}\right\}, \quad (44a)$$

where r_1 is the actual radius of the sphere, and the cutoff radius R_0 is so placed that $r_1/R_0=\frac{1}{3}$. On the other hand, at 1000 MeV the momentum transfer was large enough to allow the use of the original form Eq. (44), i.e., corresponding to $r_1=R_0$ in Eq. (44a).

V. RESULTS FOR NUCLEAR MODELS

The prediction of elastic cross sections in the high-energy approximation is based on:

(1) Determination of the potential integral function $\chi(b)$ by means of Eqs. (22), (31), or (41),

(2) Evaluation by means of Eq. (49) of the model-independent Coulomb portion of Eq. (21), corresponding to $b\geq R_0$, and

(3) Numerical integration of the model-dependent integral Eq. (47) for $b\leq R_0$.

For those physical models where $\chi(b/R_0)$ must be obtained by numerical integration of Eq. (41), it should be noted that when once this computation has been carried out for a given charge distribution, the resulting function may be stored and used repeatedly as the size of the nucleus is varied, provided only that the characteristic nuclear radius and the charge cutoff radius are scaled proportionately. Furthermore, since $\chi(b/R_0)$ for a particular model is a linear function of nuclear charge Z, it need be integrated only once for all the elements. It is of course likewise independent of energy.

The differential cross section for elastic scattering of extremely relativistic electrons or positrons from a given nuclear model is given by

$$d\sigma/d\Omega=|M|^2=|I_1+I_2|^2\cos^2(\theta/2)\,. \quad (52)$$

I_2 is obtained from Eq. (49) by employing the asymptotic expansion Eq. (A5). The resulting expression, incorporating the three lead terms of Eq. (A5) for $S_{\mu\nu}$, is

$$\mathrm{Re}I_2=\frac{kR_0}{q}[2\alpha ZAJ_0(qR_0)-DJ_1(qR_0)], \quad (53)$$

$$\mathrm{Im}I_2=\frac{kR_0}{q}[2\alpha ZBJ_0(qR_0)+CJ_1(qR_0)], \quad (54)$$

where

$$A=\frac{1}{qR_0}\left[1+\frac{4(\alpha Z)^2}{(qR_0)^2}\left\{1-\frac{4}{(qR_0)^2}[5-(\alpha Z)^2]\right\}\right], \quad (55)$$

$$B=-\frac{4\alpha Z}{(qR_0)^3}\left[1-\frac{8}{(qR_0)^2}\{1-2(\alpha Z)^2\}\right], \quad (56)$$

$$C=\frac{4(\alpha Z)^2}{(qR_0)^2}\left[1-\frac{4\{1-(\alpha Z)^2\}}{(qR_0)^2}\right], \quad (57)$$

$$D=-\frac{32(\alpha Z)^3}{(qR_0)^4}. \quad (58)$$

Since I_2 may be written

$$I_2=kR_0^2F_2^{(Z)}(qR_0)\,, \quad (59)$$

the model-independent Coulomb function $F_2^{(Z)}(qR_0)$ may be plotted for a given target element as a function only of qR_0 and applied as needed for all models and all energies. However, when a computer is used in the evaluation there is no particular advantage in this, since it is easy enough to recompute each time.

The numerical integration of Eq. (47) to obtain I_1 for energies of several hundred MeV was carried out by Simpson's rule, using 200 intervals. Test calculations were also made at 100 and in some cases at 400 intervals to verify that rounding and truncation errors of integration were not significant. The Bessel function $J_0(qR_0x)$ was stored in the computer memory for arguments <16 in the form of a table of 80 values in argument intervals of 0.2, and table look-up was employed with 4th-order interpolation. For arguments >16 the function was computed asymptotically.

The ability of the high-energy approximation to wash out the diffraction zeros first of Born approximation can be seen in Fig. 1, where the Born cross section for 420-MeV electrons scattered from a Family II (Ford-Hill model) carbon nucleus is compared with that of the high-energy approximation. The Family II charge density distribution is given by[3]

$$\begin{aligned}\rho&=\rho_0[1-\tfrac{1}{2}e^{-n(1-r/r_1)}], \quad r/r_1<1,\\ &=\rho_0[\tfrac{1}{2}e^{-n(r/r_1-1)}], \quad r/r_1>1,\end{aligned} \quad (60)$$

where

$$\rho_0=\frac{1}{4\pi r_1^3}\frac{1}{\frac{1}{3}+2/n^2+e^{-n}/n^3}.$$

In the region where the Born approximation gives good results the high-energy approximation virtually coincides with the Born cross section. In the neighborhood of the diffraction minimum, where Born approximation breaks down, the characteristic Born diffraction zero is rounded out by the infinite expansion in powers of αZ which is implicitly contained within the high-energy approximation.

The effect of this approximation is best illustrated in the case of the heavier target elements, where Born approximation becomes virtually useless. However, the effect of the reduced electron wavelength mentioned in II above should now be considered. This situation, which is common to both Born and high-energy approximations, is caused by failure to take note of the contraction of the electron's unit of length as it enters the potential well. Since the actual incident momentum k

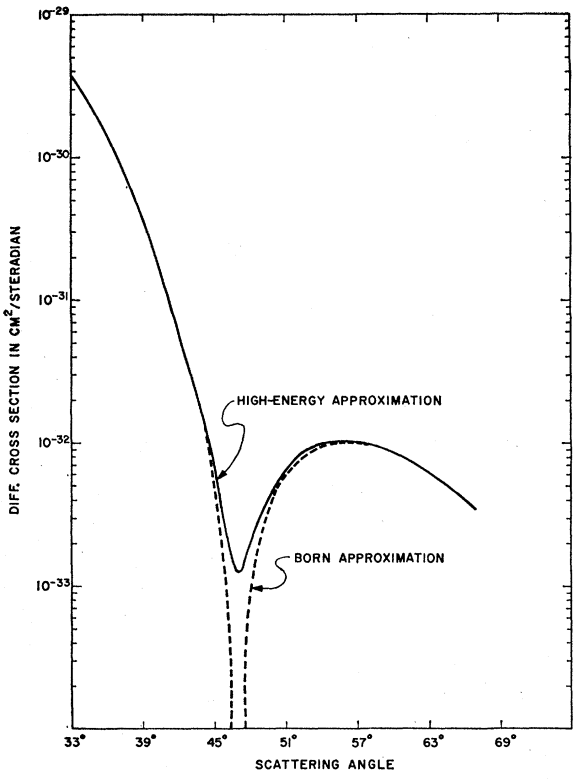

FIG. 1. Comparison of high-energy approximation and Born approximation for 420-MeV electrons scattered from carbon, Family II model, $n=4$, $r_1=2.518$ F.

Charge density $\rho=\rho_0[1-\frac{1}{2}e^{-n(1-r/r_1)}]$, $r/r_1<1$
$=\rho_0[\frac{1}{2}e^{-n(r/r_1-1)}]$, $r/r_1>1$.

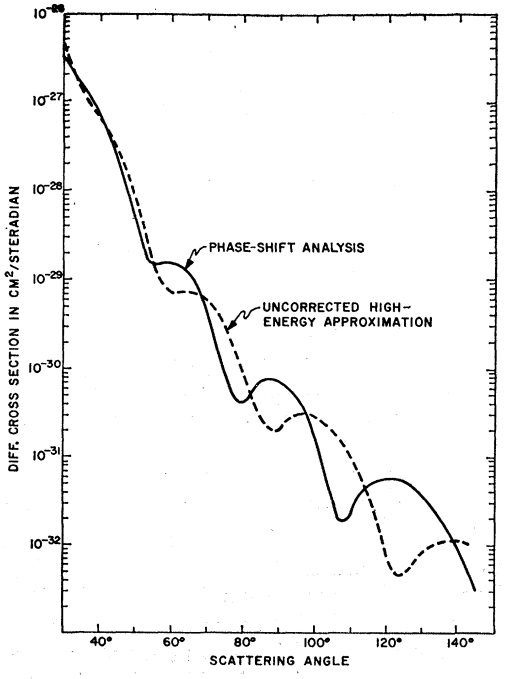

FIG. 2. Comparison of phase-shift analysis and uncorrected high-energy approximation for 241.5-MeV electrons scattered from gold, uniform model, $R=6.54$ F ($kR=8$).

is a parameter of the problem which is not confined to the vicinity of the nucleus, it may not be adjusted. Instead one describes the effect as causing the radius of the target to appear too small, shifting the diffraction pattern toward increased scattering angles. It also results in an apparent increase in the number of incident particles approaching the target per unit area, reducing the scattering cross section. This may be seen in Fig. 2, where the diffraction pattern for 241.5-MeV electrons scattered by a uniform model gold nucleus is seen to be shifted and lowered with respect to that of the phase-shift analysis results of Ravenhall and Yennie.[1,2]

Because the de Broglie wavelength actually varies continuously as the particle approaches the scattering

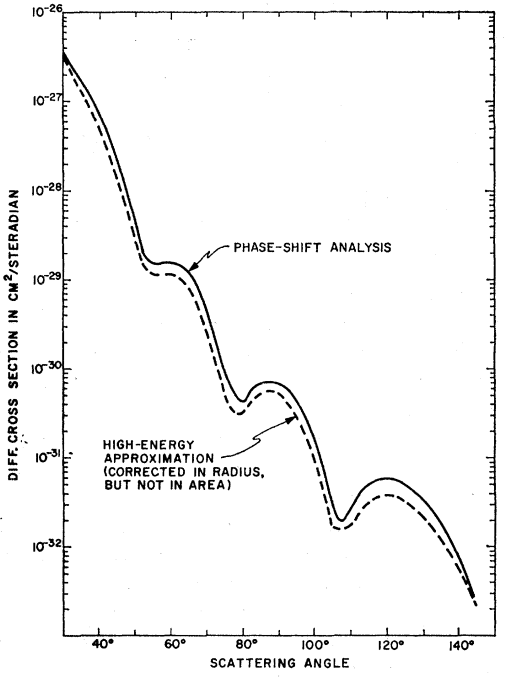

FIG. 3. Comparison of phase-shift analysis and high-energy approximation, including correction factor in radius, but not in cross section area, for 241.5-MeV electrons scattered from gold, uniform model, $R=6.54$ F ($kR=8$).

center, the failure to include this effect can be conveniently corrected only in the average sense. But since it is a small correction, and vanishes in the high-energy limit, this appears to be adequate. Conversely, an inaccuracy in application of the proper factor will merely introduce an error of the order of one or two percent in the radius predicted from fitting to experimental data.

As discussed in Sec. II we apply the factor $(1+|V|/E)$ evaluated at the rms radius to linear dimensions. In Fig. 3 this factor has been applied to the radius of the target, but no correction has been made in the cross section. Thus the pattern has been shifted in angle, but is still slightly lower than that of partial-wave analysis. This lowering effect has not been previously noticed in the case of Born approximation, due un-

doubtedly to the overpowering presence of the diffraction zeros precisely where it would otherwise be most apparent. In Fig. 4 the results have been fully corrected by the further application of the factor $(1+|V|/E)^2$ to cross sections. It may be seen that the fully corrected results are in quite close agreement with the partial wave computation.

It is interesting, and possibly significant, that after these corrections in linear dimensions, the results of the high-energy approximation are so very good, even at large scattering angles. Our argument about change of length scales is rather simple and general, although it must be admitted to have arrived after the fact.

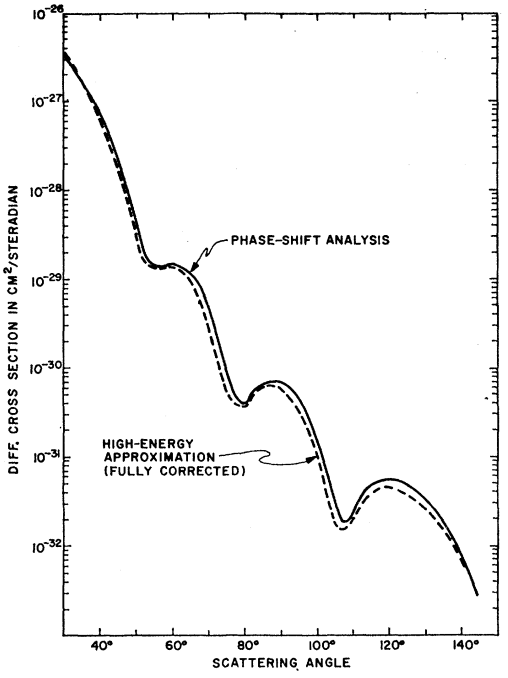

FIG. 4. Comparison of phase-shift analysis and high-energy approximation, fully corrected in both radius and cross section area, for 241.5-MeV electrons scattered from gold, uniform model, $R=6.54$ F ($kR=8$).

Since the scattering amplitude is a ratio of the number of scattered particles to the number of incident particles approaching the target per unit area, the contraction of length scales affects terms appearing in both the numerator and the denominator of this ratio. The adjustment $(1+|V|/E)$ in the nuclear radius is made to accommodate terms affecting the numerator, while the square of this factor is applied to the area term of the denominator.

In Fig. 5, 420-MeV electrons have been scattered by a Family II lead nucleus. The phase-shift analysis curves represent unpublished data from the study by Ford and Hill.[16] As an indication of some of the numerical problems two phase-shift analysis curves are plotted, corresponding to different integration intervals, for

[16] K. W. Ford and D. L. Hill, Ann. Rev. Nucl. Sci. **5**, 25 (1955).

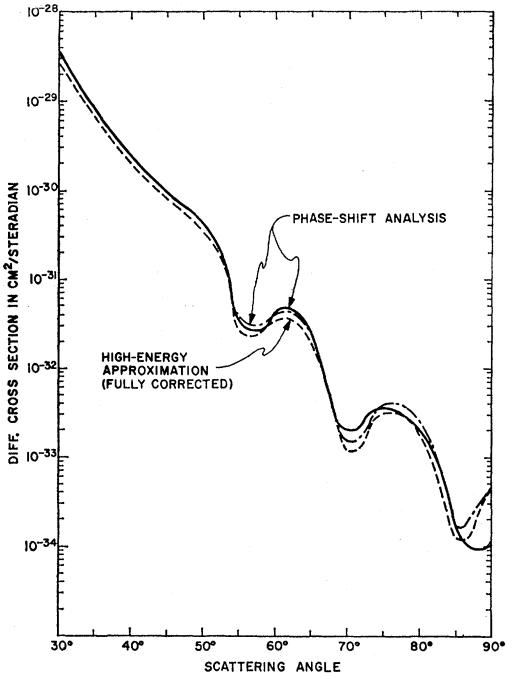

FIG. 5. Comparison of phase-shift analysis calculations based on two different integration intervals, and high-energy approximation (fully corrected). Electrons at 420 MeV scattered from lead Family II model, $n=10$, $r_1=6.67$ F.

comparison with the high-energy approximation, fully corrected. The numerical sensitivity of the phase-shift calculations can be seen at the diffraction minima, particularly at large momentum transfer, where the results become rather questionable.

Figure 6 depicts the scattering of electrons and posi-

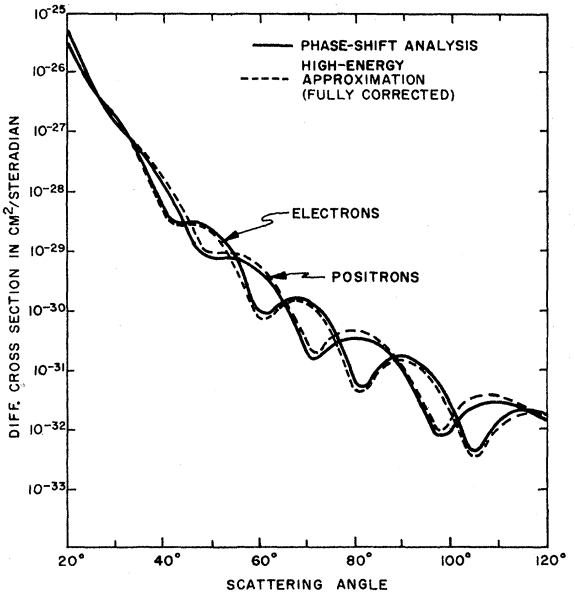

FIG. 6. Comparison of phase-shift analysis and high-energy approximation (fully corrected) for 300-MeV electrons and positrons scattered from bismuth, uniform model, $r_1=6.64$ F.

TABLE I. Correction terms $|V(r_{\text{rms}})|/E$ applied to linear dimensions for the particular targets, energies, and models considered, corresponding to "frequency modulation" of the wave function. The ratio was obtained by dividing the depth or height of the potential well or barrier, respectively, at the rms radius of the charge distribution, by the incident energy. For electron scattering the actual target radius is increased in this proportion in the calculations, while the cross section is increased by twice this amount, while for positron scattering the radius and cross section are similarly reduced.

Nucleus	Energy	Model	$\lvert V(r_{\text{rms}})\rvert/E$
Gold	241.5	Uniform	0.0935
Bismuth	300	Uniform	0.0719
Lead	420	Family II	0.0488
Carbon	420	Family II	0.0083
Gold	1000	Uniform	0.0220

trons, respectively, from bismuth at 300 MeV. The phase-shift analysis is due to Herman, Clark, and Ravenhall.[4] In the case of positron scattering the potential well becomes a barrier, and the correction changes sign, becoming $(1-|V|/E)$, so that in high-energy approximation the nuclear radius must be reduced and differential cross sections decreased. Otherwise the change in sign of the potential merely transforms Eq. (21) into its complex conjugate, producing no change in the form of the cross section. A comparison of the curves of Fig. 6 reveals the total effect of the double shift $2|V|/E$.

It appears from these results that the electron-positron difference studied by Herman, Clark, and Ravenhall is readily attributable to the effective scale change discussed above. Our calculation reveals simply and vividly what was suggested by Herman, Clark, and Ravenhall, i.e., that the electron-positron difference may be regarded as an essentially kinematic effect, probably quite insensitive to nuclear dimensions, at least at these energies.

Table I lists for the various targets, energies, and models, the appropriate rms $|V|/E$ factor applied as adjustment in radius; twice this factor was applied as corresponding correction in cross section.

A very interesting feature evident in Figs. 2 through 6 is the fact that the high-energy approximation gives excellent results for the amplitude of the diffraction oscillations. This filling in of the diffraction zeros of Born approximation to just about the right amount has not appeared in previously reported results[7] of high-energy approximations. Furthermore, it does not depend on the semiempirical change of scales correction, which merely introduces a displacement of the curves.

In view of the extent of agreement of the high-energy approximation with the results of partial-wave analysis, the former technique was applied to the scattering of electrons in the BeV energy range. This is a region in which phase-shift analysis has apparently not been practical, due to the problem of error amplification resulting from phase cancellations. It has been observed by Herman, Clark, and Ravenhall[4] in phase-shift calculations on an IBM-7090 computer with double precision arithmetic, that an attempt to distinguish certain nuclear shapes at 300 MeV was "unfortunately accompanied by the rapid decrease of both electron and positron cross sections to the 10^{-34} cm^2/sr range. At this stage even our partial-wave analysis become computationally unreliable."

To observe the behavior of the high-energy approximation under conditions of very small cross sections, a computation was carried out for scattering of 1000-MeV electrons from a uniform model gold nucleus. The results plotted in Fig. 7 show cross sections as low as 10^{-38} cm^2/sr, and are included to demonstrate the analytical capability of the technique, rather than with a view to fitting experimental data. Some 150 points were found in order to obtain this curve. The computation was found to be exceedingly stable, with very little difference in the answers between 200 and 400 integration intervals for all except the largest scattering angles, at which point the difference between 400 and 800 intervals was virtually indistinguishable. Even some probing runs at 3 BeV showed no evidence of having exceeded the capacity of the system, although finer integration intervals became necessary. Thus at high energies, precisely when the approximation becomes most valid, this technique would appear to attain its maximum usefulness.

Furthermore, it may be seen from Eqs. (47) and (48) that the scattering matrix element may be expressed in

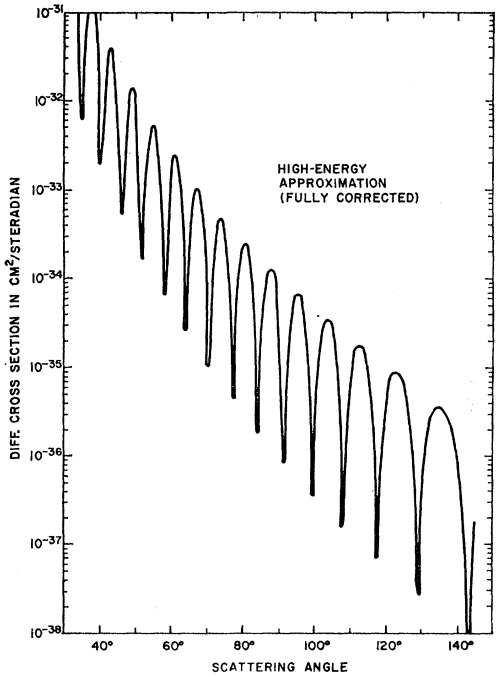

FIG. 7. High-energy approximation (fully corrected) for 1000-MeV electrons scattered from gold, uniform model, $R=6.54$ F.

the simple functional form

$$M=kR_0^2F^{(Z)}(qR_0)u_f^*u_0, \tag{61}$$

thus facilitating prediction of the effect of size and energy change on the scattering cross sections and making possible the parametrization of the results. Even for the heavier nuclei it becomes possible now to plot different energies on one curve for fitting experimental data, a procedure which in the past[3] has been confined to Born approximation.

ACKNOWLEDGMENTS

I am especially indebted to Professor Kenneth W. Ford for invaluable guidance and encouragement throughout the period of research, as well as in the preparation of this paper. The problem was suggested by Professor Ford and Professor Kirk McVoy, both of whom also introduced me to the pertinent literature of the field. Discussions at various times with Stanley Hawks contributed in providing a sounding board for some of the ideas and helpful criticism.

APPENDIX: EVALUATION OF INTEGRAL IN EQ. (48)

Integration of I_2 is difficult with the insertion of a negative damping exponential and impossible without it. It is therefore rewritten

$$I_2=I_C-I_0, \tag{A1}$$

where I_C is the pure Coulomb solution, corresponding to the integral of Eq. (48) evaluated from zero to infinity with exponential damping, and

$$I_0=\frac{kR_0^2}{i}\int_0^1 J_0(qR_0x)[e^{-2\alpha Zi\ \ln x}-1]xdx. \tag{A2}$$

As in Eq. (26),

$$I_C=\frac{2\alpha Zk}{q^2}\exp\left\{i\left[2\alpha Z\ln\frac{qR_0}{2}+2\eta\right]\right\}. \tag{A3}$$

The two terms of Eq. (A2) may be evaluated as indefinite integrals without the exponential damping factor, since the answer is the same in the limit as the factor goes to unity. The result is[12]

$$I_0=\frac{k}{iq^2}[e^{2\alpha Zi\ \ln qR_0}\{-2\alpha ZixJ_0(x)S_{-2\alpha Zi,\,-1}(x) +xJ_1(x)S_{1-2\alpha Zi,\,0}(x)\}-xJ_1(x)]_0^{qR_0}, \tag{A4}$$

where the last term in Eq. (A4) is the integral of the unity term in Eq. (A2), and the rest of the expression includes Bessel functions and Lommel's functions $S_{\mu\nu}$. The latter may be evaluated in the limit of large argument by the asymptotic series[12]

$$S_{\mu\nu}(z)\sim z^{\mu-1}\left[1-\frac{(\mu-1)^2-\nu^2}{z^2} +\frac{\{(\mu-1)^2-\nu^2\}\{(\mu-3)^2-\nu^2\}}{z^4}-\cdots\right], \tag{A5}$$

where all terms may in general be complex.

The determination of the lower limit in Eq. (A4) requires some care, since $S_{\mu\nu}(0)$ is infinite. Using a small-argument expansion[12] for $S_{\mu\nu}$, we find for small x,

$$S_{-2\alpha Zi,\,-1}(x)=\tfrac{1}{2}e^{-2\alpha Zi\ \ln 2}\Gamma(1-\alpha Zi)\Gamma(-\alpha Zi) \times[\sin\{(1-2\alpha Zi)\pi/2\}J_{-1}(x) -\cos\{(1-\alpha Zi)\pi/2\}Y_{-1}(x)], \tag{A6}$$

$$S_{1-2\alpha Zi,\,0}(x)=e^{-2\alpha Zi\ \ln 2}\Gamma(1-\alpha Zi)\Gamma(1-\alpha Zi) \times[\sin\{(1-2\alpha Zi)\pi/2\}J_0(x) -\cos\{(1-2\alpha Zi)\pi/2\}Y_0(x)], \tag{A7}$$

where $J_\nu(x)$ and $Y_\nu(x)$ are Bessel functions of the first and second kind, respectively. With the use of these expressions we find that Eq. (A4) evaluated at the lower limit is precisely equal to the negative of Eq. (A3), so that all that finally remains of I_2 is the negative of Eq. (A4) evaluated at the upper limit. Thus I_2 has the form of Eq. (49).